学位論文

Design and Control of a High-Performance Multi-Degree-of-Freedom Planar Actuator

（高性能な多自由度平面アクチュエータの設計と制御）

上田　靖人

Design and Control of a High-Performance Multi-Degree-of-Freedom Planar Actuator

by

Yasuhito Ueda

Submitted to the Department of Advanced Energy on December 12, 2008,
in partial fulfillment of the requirements for a degree of Doctor of Philosophy in Science
at the University of Tokyo

Summary

There are a large number of drive systems employing numerous actuators in industry. As such, the performances of these actuators require constant improvement in terms of higher speed and precision, miniaturization, and lower energy consumption. In addition, most of these drive systems need a design that permits MDOF (Multi-Degree-Of-Freedom) motion. Motion controls allowing MDOF have been practically realized by using stacked multiple actuators. However, there are problems in attempting to improve the performance of these types of drive systems such as a larger and more complicated structure, fluctuation of the center of gravity, and Abbe errors in position measurement due to the multiple-moving parts. In order to eliminate these problems, MDOF actuators—which have only a single moving part, but are capable of being directly driven with MDOF—are emerging technologies for future applications.

This study deals with planar actuators, which have a mover capable of traveling over large translational displacements in a plane. Various types of planar actuators have been proposed, and synchronous planar actuators with a permanent-magnet mover are expected to offer good controllability of the motion controls. However, the movable area tends to be quite narrow due to the use of conventional magnetic circuits for the MDOF drives, which are spatially separated from one another, unless the planar actuator has a large number of armature coils as shown in Figs. S-1 and S-2. Table S-1

shows classifications of synchronous planar actuators according to mover type, coil, and degree-of-freedom of controlled motion.

With this in mind, this study is aimed at designing high-performance planar actuators that have the following drive performances:

- decoupled control for 3-DOF (Three-Degree-Of-Freedom) motions on a plane.
- wide movable area that can be extended regardless of the number of armature coils.
- ease of mover miniaturization.
- no problematic wiring that can negatively influence drive performance.
- small number of armature currents to control.

Next, I propose a design for a novel synchronous planar actuator having spatially superimposed magnetic circuits for the 3-DOF drives as shown in Fig. S-3. The magnetic circuits are a combination of a two-dimensional (2-D) Halbach permanent-magnet mover, and mutually overlapped stationary polyphase armature conductors. The movable area can be easily extended by increasing the length of the armature conductors, regardless of their number. However, independently controlling MDOF driving forces by means of superimposed magnetic circuits is very difficult and an extremely important issue in this study. This thesis demonstrates a design for a planar actuator that enables MDOF driving forces to be controlled by using spatially superimposed magnetic circuits.

First, based on the results of a numerical analysis of the driving forces, I design a decoupled control law for the 3-DOF driving forces on a plane by using two polyphase armature currents. I experimentally demonstrate that the 3-DOF motions of the mover can be independently controlled by using two polyphase armature currents. The movable area in the translational directions is infinitely wide, and that in the yaw direction is in the range within ± 26 deg, namely the planar actuator has the widest movable area of all planar actuators that have only two polyphase armature conductors. Second, in order to further improve drive characteristics, the planar actuator is theoretically redesigned so that the mover can be stably levitated and the 3-DOF motions above a plane can be controlled. The planar actuator can be made quite small because the permanent-magnet array and armature conductors for the MDOF drive are integrated. The planar actuator would provide a significant starting point when used with small electromechanical components in an MDOF drive.

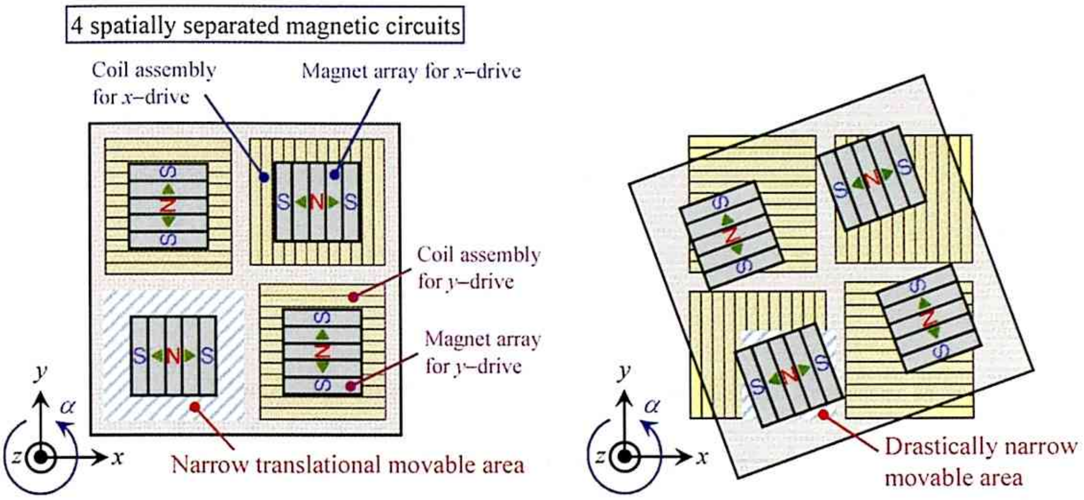

(a) When not displaced in the yaw direction. (b) When displaced in the yaw direction.

Fig. S-1: Configuration of a fundamental synchronous planar actuator with a permanent-magnet mover. The movable area tends to be quite narrow.

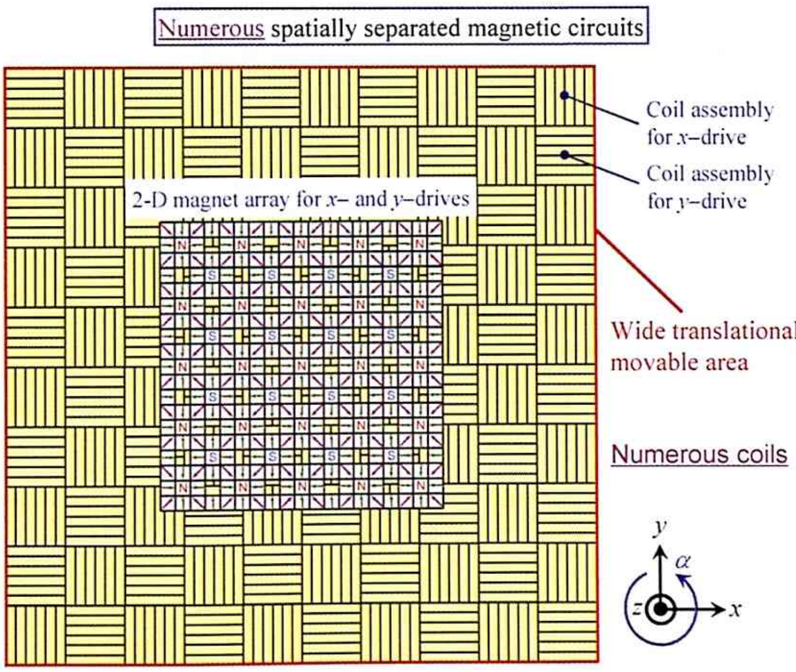

Fig. S-2: Configuration of a synchronous planar actuator with a permanent-magnet mover and numerous armature coils. The power-supply system often becomes complex.

Table S-1: Classification of synchronous planar actuators by mover type, coil, and degree-of-freedom of controlled motion.

Coil Type \ Mover Type	Moving-Magnet Type No problematic wiring			Moving-Coil Type Extendible movable area regardless of number of coils		
	Inventor	DOF	Coils	Inventor	DOF	Coils
Polyphase Coils Less dependence of driving forces on mover positions	Korenaga	2	$2 \times 2\phi$	Hinds	3	$4 \times 6\phi$
	Fujii	2	$2 \times 3\phi$	Jung	3	$4 \times 3\phi$
	Ohira	5	$2 \times 3\phi$ (+ 4)	Shikayama	3	$4 \times 3\phi$
				Compter	6	$4 \times 3\phi$
	Kim	6	$4 \times 3\phi$			
	Compter	6	$9 \times 3\phi$			
	Oh	6	$100 \times 3\phi$			
	Ueda	3	$2 \times 3\phi$			
	(This study)	5	$3 \times 2\phi$			
Non-Polyphase Coils High design flexibility	Binnard	3	Many	Asakawa	3	4
	Ueta	3	Many	Ueta	6	Many
	Vandenput	6	84			

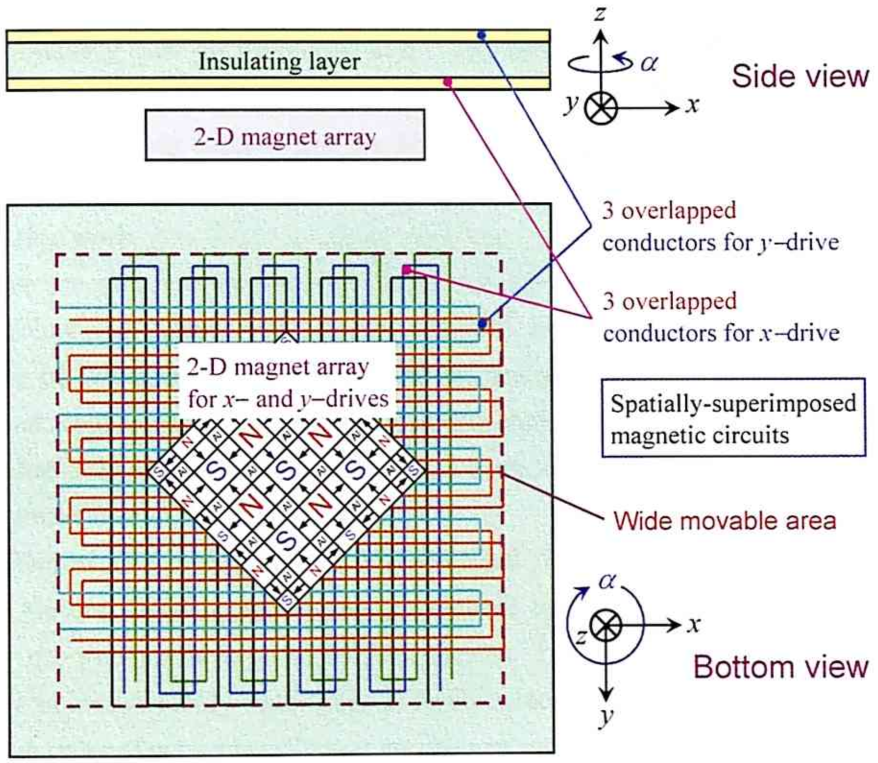

Fig. S-3: Configuration of proposed synchronous planar actuator with a permanent-magnet mover and a small number of armature coils.

Acknowledgments

First of all, I would like to thank my supervisor, Prof. Hiroyuki Ohsaki, for his careful and consistent support. I remember being impressed by the potential of high-performance dynamics offered by using MDOF actuators when he suggested this challenging research. This study covers a wide range of fields including electric machinery, electromagnetics, control theory, mechanics, and precision measurements. Furthermore, MDOF physical phenomena, which are intricately linked, often presented me with uniquely difficult problems, and I was seriously puzzled at various stages in this work. However, Prof. Ohsaki has a wide range of knowledge, physical intuition, and the kindness to eagerly support this project, and his support in various aspects was very helpful in this research. Thanks to his consistent support, I managed to successfully complete this work.

During the preliminary deliberation of this Ph. D. thesis, Prof. Yoichi Hori, Prof. Akihiko Yokoyama, Assoc. Prof. Takafumi Koseki, and Assoc. Prof. Jumpei Baba of the University of Tokyo, made significant and pertinent comments, and offered criticism, advice, and viewpoints. They pointed out incomplete points in the thesis, and this helped to logically and technically enrich this work. I am extremely appreciative of their diligence and I would like to thank them.

The Technical Committee on Systematized Technologies of Multi Degrees of Freedom Motors, IEEJ, gave me many excellent opportunities to join discussions on research into and application of MDOF devices. The members of the committee are specialists in an extremely wide range of fields related to MDOF drive systems, such as the various types of actuators, electric machinery, mechanics, motion control, precession engineering, robotics, magnetic materials, sensing technologies, mechanical suspensions, and applications. In the committee, the members all contribute and discuss the latest topics of research and development in these diverse fields. Through several discussions in the committee, I was able to achieve not only self-improvement in my knowledge of these fields, but also acquire consistent comments on my study and approaches for solving various difficult problems. So here again, I am extremely appreciative of their diligent work, and would like to thank the members of the committee: Dr. Tomoaki Yano, Advanced Industrial Science and Technology; Prof. Daiki Ebihara and Prof. Hideo Dohmeki, Musashi, Institute of Technology; Mr. Toshihiko Watanabe, IEEJ Professional; Mr. Eiji Oi, Oriental Motor Co., Ltd.; Dr. Mitsuji Karita, Japan Science and Technology Agency; Prof. Hiroyuki Wakiwaka, Shinshu University; Prof. Shinji Wakui, Tokyo University of Agriculture and Technology; Mr. Atsushi Horikoshi, NSK Ltd.; Dr. Yoshiyuki Tomita, Sumitomo Heavy Industries Co., Ltd.; Prof. Katsuhiro Hirata, Osaka University; Assoc. Prof. Koichi Oka, Kochi University of Technology; Assoc. Prof. Shigeri Inui, Nihon University; and Assist. Prof. Junichi Tsuchiya, Tokyo Metropolitan University.

With regard to conferences, symposiums, workshops and other such occasions, I would like to thank a large number of researchers for their consistent and helpful comments and advice, in particular Dr. Mimpei Morishita, Toshiba Co., Ltd.; Prof. A. J. A. Vandenput and Dr. J. W. Jansen, Eindhoven University of Technology; Mr. Nobushige Korenaga, Canon Co., Ltd.; Prof. Gao Wei, Tohoku University; and Dr. Toru Shikayama, Yaskawa Electric Co., Ltd.

For the design and fabrication of the experimental apparatuses, I would like to thank Mr. Atsushi Saito, a technical staff member at the University of Tokyo for his careful instruction in mechanical design and machining over a period of five years. In the manufacture of the Halbach permanent magnets, Dr. Ken Ohashi, Mr. Yasuaki Aoyama, Mr. Koji Miyata and Mr. Yuji Doi, Shin-Etsu Chemical Co., Ltd. provided a great many Nd-Fe-B permanent magnets and 2-D Halbach permanent-magnet arrays prototyped for this research. They also demonstrated to me the properties of permanent magnets, and gave advice on bonding adhesive used to fabricate the 2-D Halbach permanent-magnet array. I would like to thank them for their willing provision of Nd-Fe-B magnets and careful advice.

As for my time spent in the laboratory at the University of Tokyo, I would like to thank Dr. Jaeho Kim, Advanced Industrial Science and Technology; Prof. Huang Xueliang, Southeast University, Nanjing; Asst. Prof. Dr. Masaki Sekino and Mr. Yuzuru Tamura; the secretaries Ms. Yuko Yamazaki and Ms. Yuko Nagatsuma; and, a lager number of my colleagues for their support and encouragement in numerous aspects: Mr. Dong-Min Kim, Mr. Akihisa Miyazoe, Mr. Yoshiki Komi, Mr. Tatsuya, Suzuki, Mr. Yutaka Terao, Mr. Souhei Nonaka, Mr. Hitoshi Yasuda, Mr. Takeshi Ikenaga, Mr. Masahiro Yamada, Mr. Satoshi Tatara, Mr. Shinji Wasada, Mr. Ryosuke Shiraishi, Dr. Yota Ichiki, Mr. Satoshi Kawamoto, Mr. Masaki Hashimoto, Mr. Yukihiro Hattori, Mr. Xiao-Fei Qian Mr. Toshiyuki Hirota, Mr. Sousuke Matsumura, Mr. Maurice Nibelle, Mr. Souichiro Bando, Mr. Takeshi Nagayama, Mr. Masashi Fujimoto, Dr. Jian Du, Mr. Yasunori Kawamoto, Mr. Keita Fujiyama, and Mr. Kozo Ohira.

Finally, I would like to thank my lovely family very much for taking care of me ever since the time I was born. They have supported me physically, mentally, and

economically in my life for a long time. Thanks to their kind support, I have had quite a happy life, and I am extremely appreciative of their kindness.

Contents

List of Figures

List of Tables

List of Symbols

a	side of square mover (m) or first element of displacement vector $\boldsymbol{d}_t$ (m)
$\boldsymbol{B}$	vector of flux density (T)
B	flux density (T)
$(BH)_{max}$	maximum magnetic energy product (kJ/m^3)
B_r	residual flux density (T)
B_x	flux density in x–direction (T)
B_y	flux density in y–direction (T)
B_z	flux density in z–direction (T)
B_{zm}	maximum flux density in z–direction due to magnet arrays dealt with in this study (T)
B_{zm1}	maximum of flux density B_{z1} (T)
B_{zm2}	maximum of flux density B_{z2} (T)
B_{z0}	maximum flux density in z–direction due to magnet array shown in Fig. 3.1.2-1 (T)
B_{z1}	flux density in z–direction due to Jung's proposed magnet array (T)
B_{z2}	flux density in z–direction due to Compter's proposed magnet array (T)
b	second element of displacement vector $\boldsymbol{d}_t$ (m)
c	third element of displacement vector $\boldsymbol{d}_t$ (m)
$\boldsymbol{D}_F$	differential parameters of PID controller for translational force (Ns/m)
D	reference distance of laser-displacement sensor (m)
$D_{T\alpha}$	differential parameters of PID controller for torque (1/s)
$\boldsymbol{d}_t$	displacement vector (m)
$d\boldsymbol{F}$	vector of translational force acting on line element dl_{jk} (N)
db_4	distance between sensor head and measurement point in Sensors 4 (m)
db_5	distance between sensor head and measurement point in Sensors 5 (m)
db_6	distance between sensor head and measurement point in Sensors 6 (m)
dl_{jk}	line element of armature conductor l_{jk} (m), where j (= x or y) and k (= u, v, or w) express driving direction and phase name of three-phase currents, respectively
$d\boldsymbol{T}$	vector of torque acting on line element dl_{jk} (N·m)
dt	time step in motion analysis (s)
$\boldsymbol{E}$	unit matrix
$\boldsymbol{F}$	vector of translational force with respect to stationary coordinate (N)

$\boldsymbol{F}_g$	forces of gravity acting on mover (N)
$\boldsymbol{F}_L$	Lorentz force (N)
$\boldsymbol{F}_{sm}$	vector of translational force with respect to stationary coordinate (N)
F_x	translational force in x_s–direction (N)
F_y	translational force in y_s–direction (N)
F_z	translational force in z_s–direction (N)
g	acceleration of gravity (m/s^2)
H	intensity of magnetic field (A/m)
H_c	coercive force (A/m)
h	height of mover (m)
I_c	current limit (A)
I_j	amplitude of three-phase current (A), where j (= x, y, or α) expresses driving direction
I_{1j}	first two-phase current (A), where j (= x, y, or α) expresses driving direction
I_{2j}	second two-phase current (A), where j (= x, y, or α) expresses driving direction
I_{dj}	direct-axis current (A), where j (= x, y, or α) expresses driving direction
I_{qj}	quadrature-axis current (A), where j (= x, y, or α) expresses driving direction
I_0	amplitude of three-phase current (A)
$\boldsymbol{i}$	vector of armature current (A)
$\boldsymbol{i}_j$	two-phase armature current (A), where j (= x, y, or α) expresses driving direction
$\boldsymbol{i}_{jk}$	vector of armature current (A), where j (= x or y) and k (= u, v, or w) express driving direction and phase name of three-phase current, respectively
i_{ju}	first three-phase armature current (A), where j (= x or y) expresses driving direction
i_{jv}	second three-phase armature current (A), where j (= x or y) expresses driving direction
i_{jw}	third three-phase armature current (A), where j (= x or y) expresses driving direction
i_k	three-phase armature current in basic coreless linear synchronous motor (A), where k (= u, v, or w) expresses driving direction
$\boldsymbol{J}_m'$	inertia tensor of mover with respect to mover coordinate $x_m y_m z_m$ (kg·m^2)
$\boldsymbol{J}_s'$	inertia tensor of mover with respect to stationary coordinate $x_s y_s z_s$ (kg·m^2)
$\boldsymbol{J}_O'$	inertia tensor of rectangular prism with respect to stationary coordinate $x_s y_s z_s$ (kg·m^2)
$\boldsymbol{J}_{Ot}'$	inertia tensor rectangular prism with respect to coordinate $x_t y_t z_t$ (kg·m^2)

J_{jk}'	element of inertia tensor of mover (kg·m^2), where j and k (= x, y, or z) express mover-coordinate axes
$\boldsymbol{K}$	6 × 6 matrix of system constant (N/A or N·m/A)
$\boldsymbol{K}_{FT}$	6 × 4 matrix of system constant (N/A or N·m/A)
K_{FC}	approximated system constant (N/A)
K_{Fx}	system constant in translational force due to armature current for x–directional drive (N/A)
K_{Fy}	system constant in translational force due to armature current for y–directional drive (N/A)
K_{TC}	approximated system constant (N·m/A)
K_{TP}	approximated system constant per rotational angle (N·m/rad·A)
K_{Tx}	system constant in torque due to armature current for x–directional drive (N·m/A)
K_{Ty}	system constant in torque due to armature current for y–directional drive (N·m/A)
K_{ab}	$a \times b$ element of matrix of system constant (N/A or N·m/A), where a and b are 1, 2, 3, 4, 5, or 6
K_u	magnetic anisotropic energy (MJ/m^3)
l	length of mover (m)
l_{jk}	armature conductor, where j (= x or y) and k (= u, v, or w) express driving direction and phase name of three-phase current, respectively
l_x	length of first edge of rectangular prism (m)
l_y	length of second edge of rectangular prism (m)
l_z	length of third edge of rectangular prism (m)
$\boldsymbol{M}_i$	infinitesimal rotation generator, where i is 1, 2, or 3
M	magnetic polarization (A/m) or mass of mover (kg)
M_r	residual magnetic polarization (A/m)
M_s	saturation magnetic polarization (A/m)
N_i	positive number
$\boldsymbol{n}_{msi,0}$	normal vector $\boldsymbol{n}_{msi}$ when mover is not displaced from base position
$\boldsymbol{n}_{msi}$	normal vector of surface i with respect to sensor coordinate $x_l y_l z_l$, where i is 1, 2, 3, 4, 5, or 6
n	number of armature conductors
O	origin of stationary coordinate or origin of laser coordinate
O'	origin of mover coordinate
$\boldsymbol{P}_F$	proportional parameters of PID controller for translational force (N/m)

$P_{T\alpha}$	proportional parameters of PID controller for torque (1/s^2)
$\boldsymbol{R}$	rotational matrix
$\boldsymbol{R}_{lm}$	orientation of mover with respect to laser coordinate $x_ly_lz_l$
$\boldsymbol{R}_{ms}$	orientation of stationary coordinate $x_sy_sz_s$ with respect to mover coordinate $x_my_mz_m$
$\boldsymbol{R}_{sl}$	orientation of laser coordinate $x_ly_lz_l$ with respect to stationary coordinate $x_sy_sz_s$
$\boldsymbol{R}_{sm}$	orientation of mover coordinate $x_my_mz_m$ with respect to stationary coordinate $x_sy_sz_s$
$\boldsymbol{R}_{s1}$	rotation matrix from stationary coordinate $x_sy_sz_s$ to coordinate $x_1y_1z_1$
$\boldsymbol{R}_{\omega\phi}$	3×3 matrix relating angular velocity to differential of Euler angle
$\boldsymbol{R}_{\psi}$	rotational matrix as ψ counterclockwise rotation about rotational vector $\boldsymbol{\lambda}$
$\boldsymbol{R}_{12}$	rotation matrix from coordinate $x_1y_1z_1$ to coordinate $x_2y_2z_2$
$\boldsymbol{R}_{2m}$	rotation matrix from coordinate $x_2y_2z_2$ to mover coordinate $x_my_mz_m$
R	resistance of armature conductor (Ω)
$\boldsymbol{r}$	position vector from rotation center with respect to mover-coordinate axes (m)
$\boldsymbol{r}_i$	vector of initial position of mover (m)
$\boldsymbol{r}_{jk}$	position vector of line element dl_{jk} (m)
$\boldsymbol{r}_{li}$	path of laser beam from Sensor i with respect to sensor coordinate $x_ly_lz_l$ (m), where i is 1, 2, 3, 4, 5, or 6
$\boldsymbol{r}_{lm}$	mover position with respect to laser coordinate $x_ly_lz_l$ (m)
$\boldsymbol{r}_{lsi}$	position vector of arbitrary point on a surface i with respect to the sensor coordinate $x_ly_lz_l$, where i is 1, 2, 3, 4, 5, or 6
$\boldsymbol{r}_{msi,0}$	position vector $\boldsymbol{r}_{msi}$ when mover is not displaced from base position (m)
$\boldsymbol{r}_{msi}$	position vector of center of surface i with respect to sensor coordinate $x_ly_lz_l$, where i is 1, 2, 3, 4, 5, or 6 (m)
$\boldsymbol{r}_m$	position vector of mover center (m)
$\boldsymbol{r}_{sm}$	position vector of mover with respect to stationary coordinate $x_sy_sz_s$ (m)
r	radial coordinate (m)
S_1	output signal of laser-displacement sensor 1 (m), commuted from voltage signal to position signal
S_2	output signal of laser-displacement sensor 2 (m), commuted from voltage signal to position signal
S_3	output signal of laser-displacement sensor 3 (m), commuted from voltage signal to position signal
$\boldsymbol{T}$	vector of torque with respect to stationary coordinate (N·m)
$\boldsymbol{T}_{sm}'$	vector of torque with respect to mover coordinate (N·m)

T_x	torque around x_s–axis (N·m)
T_x'	torque around x_m–axis (N·m)
T_{xa}'	torque due to armature currents $\boldsymbol{i}_x$ and $\boldsymbol{i}_y$ around x_m–axis (N·m)
T_y	torque around y_s–axis (N·m)
T_y'	torque around y_m–axis (N·m)
T_z	torque around z_s–axis (N·m)
T_z'	torque around z_m–axis (N·m)
T_{za}'	torque due to armature currents $\boldsymbol{i}_x$ and $\boldsymbol{i}_y$ around z_m–axis (N·m)
T_c	Curie temperature (°C)
t	time in experiment or analysis (s)
t_c	control period (s)
V	volume of mover (m^3)
v_{sm}	velocity vector of mover with respect to stationary coordinate (m/s)
v_{jk}	armature voltage (V), where j (= x or y) and k (= u, v, or w) express driving direction and phase name of three-phase current, respectively
w	width of mover
X_1	x–position of measurement point of Sensor 1 (m)
x	first coordinate (m)
x_l	first coordinate of 2-D Halbach permanent-magnet array (m) or first laser coordinate (m)
x_m	first mover coordinate (m)
x_s	first stationary coordinate (m)
x_α	first coordinate of armature conductors for α–directional drive (m)
x_0	position of multipole permanent-magnet array (m)
x_1	first immediate coordinate after first rotation (m)
x_{12}	relative distance between Sensor 1 and Sensor 2 in x–direction (m)
x_2	first immediate coordinate after second rotation (m)
x_{23}	relative distance between Sensor 2 and Sensor 3 in x–direction (m)
x_{45}	relative distance between Sensor 4 and Sensor 5 in x–direction (m)
Y_2	y–position of measurement point of Sensor 2 (m)
Y_3	y–position of measurement point of Sensor 3 (m)
y	second coordinate (m)
y_{L1}	first length defined by Fig. C-3
y_{L2}	second length defined by Fig. C-3
y_l	second coordinate of 2-D Halbach permanent-magnet array (m) or second laser coordinate (m)

y_m	second mover coordinate (m)
y_s	second stationary coordinate (m)
y_α	second coordinate of armature conductors for α–directional drive (m)
y_1	second immediate coordinate after first rotation (m)
y_{12}	relative distance between Sensor 1 and Sensor 2 in y–direction (m)
y_2	second immediate coordinate after second rotation (m)
y_{23}	relative distance between Sensor 2 and Sensor 3 in y–direction (m)
y_{56}	relative distance between Sensor 5 and Sensor 6 in y–direction (m)
z	third coordinate (m)
z_l	third laser coordinate (m)
z_m	third mover coordinate (m)
z_s	third stationary coordinate (m)
z_1	third immediate coordinate after first rotation (m)
z_2	third immediate coordinate after second rotation (m)
α	yaw angle (rad) or first Euler angle (rad)
α_l	first Euler angle defined by rotations around z_l–, y_l–, and x_l–axes (rad)
$\alpha_l^{'}$	tilted angle about z_l–axis in $x_l - y_l$ plane (rad)
$\alpha_{\min}$	yaw angle defined by Eq. (4.2.2-1) (rad)
$\alpha_{\max}$	yaw angle defined by Eq. (4.2.2-2) (rad)
α_s	phase of magnetic field due to magnet mover for α–directional drive (m)
α_0	yaw angle defined by Eq. (6.1.2-1) (rad)
β	pitch angle (rad) or second Euler angle (rad)
β_l	second Euler angle defined by rotations around z_l–, y_l–, and x_l–axes (rad)
$\beta_l^{'}$	tilted angle of mover to $x_l - y_l$ plane about y_l–axis (rad)
ΔS_4	displacement in measurement point of Sensor 4 from base position (mm)
ΔS_5	displacement in measurement point of Sensor 5 from base position (mm)
ΔS_6	displacement in measurement point of Sensor 6 from base position (mm)
δ_{jk}	Kronecker delta, where j and k (= x, y, or z) express mover-coordinate axes
γ	roll angle (rad) or third Euler angle (rad)
γ_l	third Euler angle defined by rotations around z_l–, y_l–, and x_l–axes (rad)
$\gamma_l^{'}$	tilted angle about x_l–axis in cross-section B–B' shown in Fig. C-3 (rad)
$\boldsymbol{\phi}$	vector of Euler angle (rad)
$\boldsymbol{\phi}_i$	vector of initial Euler angle (rad)
$\boldsymbol{\phi}_l$	vector of Euler angle defined by rotations around z_l–, y_l–, and x_l–axes (rad)
ϕ	electrical phase

φ	tilted angle of armature conductors for α–directional drive from those for x–directional drive (rad)
λ	rotational vector
λ_{lx}	unit vector of x_s–axis with respect to laser coordinate $x_l y_l z_l$
λ_{ly}	unit vector of y_s–axis with respect to laser coordinate $x_l y_l z_l$
λ_{ms}	unit vector of x_s–axis with respect to coordinate $x_2 y_2 z_2$
λ_{1s}	unit vector of z_s–axis with respect to stationary coordinate $x_s y_s z_s$
λ_{2s}	unit vector of y_s–axis with respect to coordinate $x_1 y_1 z_1$
θ_s	phase of three-phase current (rad)
θ_{sj}	phase of three-phase current (rad), where j (= x, y, or α) expresses driving direction
θ_{dj}	phase difference between magnetic fields generated by armature conductors and mover (rad), where j (= x, y, or α) expresses driving direction
θ_4	tilted angle of laser beam from Sensors 4 to z_l–axis (rad)
θ_5	tilted angle of laser beam from Sensors 5 to z_l–axis (rad)
θ_6	tilted angle of laser beam from Sensors 6 to z_l–axis (rad)
ρ	mass density of mover (kg/m^3)
τ	length of pitch of planar actuator (m)
τ_{PM}	length of pole pitch due to 2-D Halbach permanent-magnet array in x_l– or y_l–directions (m)
τ_0	length of pitch of multipole permanent-magnet array (m)
ω_{sm}'	angular velocity of mover with respect to mover coordinate (rad/s)
χ	magnetic susceptibility
ψ	rotational angle (rad)

In this thesis, superscript "*" and subscript "$_{ref}$" indicate reference signal.

Chapter 1

Introduction

This chapter introduces the background to this study, which includes general features, element technologies, and technical issues related to MDOF actuators. Next, the purpose and position of this study against this background, and the contribution of this thesis are presented.

1. Introduction

Conventionally, linear drives have been realized by a combination of rotary motors and reduction gears. Continual advances are being made to improve the speed of the drives and the precision of the positioning of motion controls, however, these drive systems have extremely complicated nonlinear phenomena such as friction and backlash, which makes it difficult to attain satisfactory drive performance. Against this background, direct drives have been attracting attention because they are high-performance drives that do not use reduction gears, and drive systems utilizing linear motors have replaced drive systems that use a combination of rotary motors and reduction gears in industry applications, for example in robots and machine tools.

Most industry applications require that drive systems be able to control MDOF motion. Motion controls with MDOF have to date been practically realized by stacking multiple linear motors. Looking ahead, MDOF actuators, which have only a single mover capable of being directly driven in MDOF, are emerging technologies for the future. MDOF actuators offer the following advantages: the center of mass of the mover does not fluctuate, easier creation of smaller structure, and a saving on energy consumption [MDD05].

This chapter introduces the general features, element technologies, and technical issues of MDOF actuators. Next, the purpose and position of this study against this background, and the contribution of this thesis are presented.

1.1. Actuators with MDOF

In an MDOF drive system built using stacked rotary and linear motors (one-degree-of-freedom, or 1-DOF, drive), the motor on the lower side of the drive system requires a high degree of torque to suspend the mass of the motor on the upper side of the drive system. Consequently the drive system tends to have a much larger structure than the load of its drive system [MDD05]. Furthermore, these drive systems have more complicated multi-body dynamics, which make it difficult to realize high-performance motion controls. On the other hand, MDOF actuators have only a single mover, which can be directly driven with MDOF, and they are therefore expected to gain acceptance as MDOF drive systems offering a simple structure and high performance [MDD05].

Most MDOF actuators can be classified into two prominent types [MDD05]: a planar actuator that can drive in two-degrees-of-freedom (2-DOF) translational directions; and, a spherical actuator that can drive in 2-DOF rotational directions. As for the drive principles, electromagnetic, piezoelectric, magnetostrictive, and electrostatic types of MDOF actuators have been proposed. Most models are of the electromagnetic actuator type [MDD05, MDD07, MDD08].

Planar actuators have been studied with the primary objective of application in high-precision and high-speed stages in fields such as semiconductor manufacturing equipment, machine tools, and conveyance systems [MDD08]. To date, various types of planar actuators have been proposed, including stepping, induction, and synchronous types. In stepping planar actuators, the mover can be positioned without position sensors to a positioning accuracy of several tens of μm. In induction planar actuators, the mover consists of a single aluminum plate including a back iron, and the structure tends to be simple and solid. In synchronous planar actuators, the driving forces have a proportional dependence on the amplitude of polyphase current, and a sinusoidal dependence on the phase difference between the magnetic field generated by the stator and the mover. Therefore, synchronous planar actuators are often adopted because of their good controllability in terms of motion control. The mover of the planar actuator is suspended on ball bearings, air bearings, or magnetic bearings. The position of the mover is measured using a combinations of optical sensors (for example, laser interferometers, photodetectors, encoders, or 2-D angle sensors), and magnetic sensors (for example, Hall elements, or differential transformers), inductive sensors or capacitance sensors.

Spherical actuators have been studied with the primary objective of usage in robot components, for example, their joints and eyes [MDD08]. Various types of planar actuators have been proposed including stepping, induction, synchronous, piezoelectric, and magnetostrictive models. The driving forces of electromagnetic spherical actuators (that is to say, stepping, induction, and synchronous types) have the same features as planar actuators. However, it is very difficult to suspend the mover and to sense position.

Piezoelectric actuators can drive the mover in close contact with the stator by controlling the piezoelectric strain on the stator, which is made of a piezoelectric material [Act04]. Piezoelectric actuators are generally small (less than several-cm in size), and can generate high-power driving forces and retaining forces with the power supply turned off. Therefore, piezoelectric actuators are suitable for small actuators used for short-stroke precise positioning. The mover is often precompressed by electromagnetic forces so that the mover is in close contact with the stator.

Magnetostrictive actuators drive the mover in close contact with the stator by controlling the magnetostrictions of the stator, which is a magnetic material [Hig07]. Magnetostrictive actuators often have superior temperature characteristics and mechanical characteristics to those of piezoelectric actuators [Hig08a].

In electrostatic actuators, the driving force (electrostatic forces) per volume (unit: m^3) is inversely proportional to their length (unit: m) [Act04]. When the dimensions of electrostatic actuators decrease, the driving force per mover weigh increases. Therefore, electrostatic actuators are being studied for use in micro-electro-mechanical systems (MEMS). In addition, high-power electrostatic actuators having dimensions of a few cm can be realized by integrating micro-electrostatic actuators. To generate a sufficient driving force, however, it is necessary to supply several kV of power across the gap between the moving and stationary electrodes, which is a sub-mm gap, and to design electrostatic actuators that are not subject to dielectric breakdown.

1.2. Element Technologies of MDOF Actuators

To construct MDOF actuators, various technologies such as driving force generation, position sensing, and suspension and guide mechanisms are absolutely essential [MDD07]. First, driving forces with some degree of freedom need to be independently generated. Second, the mover position in all driving directions needs to be detected precisely within a short time period. Finally, the mover motion—except in the driving directions—should be constrained, having less influence on the mover motion in the driving directions. In electromagnetic actuators with MDOF, the performance of the driving forces depends on the characteristics of the magnetic material used and the configuration of the magnetic circuits. This section introduces element technologies of electromagnetic MDOF actuators such as magnetic materials, magnetic circuits, position-sensing methods, and suspension and guide mechanisms.

1.2.1. Magnetic Materials

Most electromagnetic actuators with MDOF make use of permanent magnets to achieve both a compact structure and high-power driving forces [MDD05, MDD07]. Thus, permanent magnets are essential for these actuators, and they are created by magnetizing magnetic materials. The magnetic characteristics of these magnetic materials are vitally important in the design of high-performance actuators.

As we know, ferromagnetic materials polarize in a magnetic field H. Figure 1.2.1-1 shows the magnetic polarization M, and flux density B, of a ferromagnetic material when the material is positioned in the magnetic field H; the M–H curve and B–H curve have hysteretic properties. In Fig. 1.2.1-1, the residual flux density, coercive force, residual magnetic polarization, saturation magnetic polarization, and magnetic susceptibility are expressed as B_r, H_c, M_r, M_s, and χ, respectively [Sag07].

To evaluate the performance of a permanent magnet, a maximum energy product $(BH)_{max}$ is often utilized, which expresses the maximum magnetic energy stored in a permanent magnet, and depends on the residual flux density B_r and coercive force H_c. Rare-earth magnets, which are alloys with rare-earth metals and 3d transition metals, have the highest $(BH)_{max}$ of all known permanent magnets [Edw01, Sag07, Taw05]. To date, rare-earth magnets in which the main phase is $SmCo_5$, Sm_2Co_{17}, $Nd_2Fe_{14}B$, or $Sm_2Fe_{17}N_3$ have been presented [Fuk04]. Table 1.2.1-1 shows the magnetic characteristics and theoretical limitations of $(BH)_{max}$ of alloys with rare-earth and a transition metal [Fuk04]. Table 1.2.1-1 shows that a $Nd_2Fe_{14}B$ magnet has a maximum limitation of $(BH)_{max}$. In fact, a $Nd_2Fe_{14}B$ magnet in which the $(BH)_{max}$ is more than 400 kJ/m^3 has been reported, and the $(BH)_{max}$ is developed further every year as shown in Fig, 1.2.1-2 and is close to the theoretical limit [Kan04].

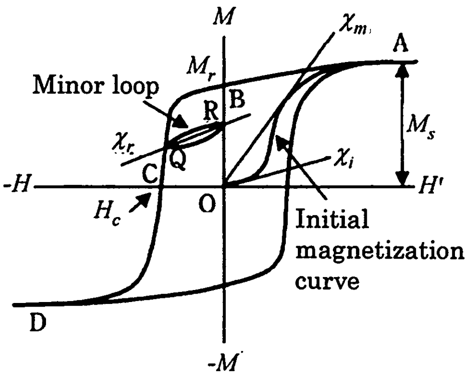

(a) Hysteresis curve

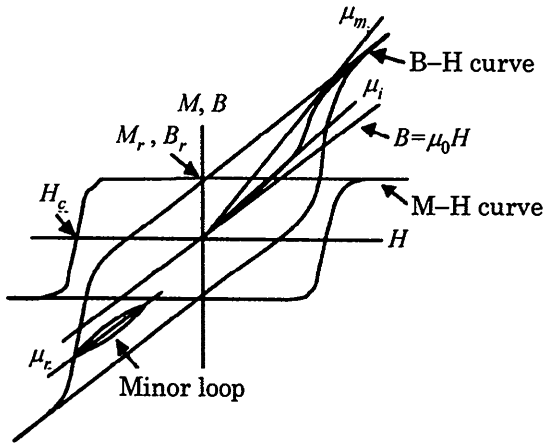

(b) M–H curve and B–H curve

Fig. 1.2.1-1: Magnetic characteristics of ferromagnetic materials [Sag07].

Table 1.2.1-1: Magnetic characteristics of rare-earth magnets [Fuk04].

Material	M_s (T)	K_u (MJ/m^3)	T_c (°C)	$(BH)_{max}$ (KJ/m^3)
$SmCo_5$	1.14	11–20	727	259
Sm_2Co_{17}	1.25	3.2	920	311
$Nd_2Fe_{14}B$	1.60	4.5	313	509
$Sm_2Fe_{17}N_3$	1.57	21	474	490

K_u : Magnetic anisotropic energy, T_c : Curie temperature

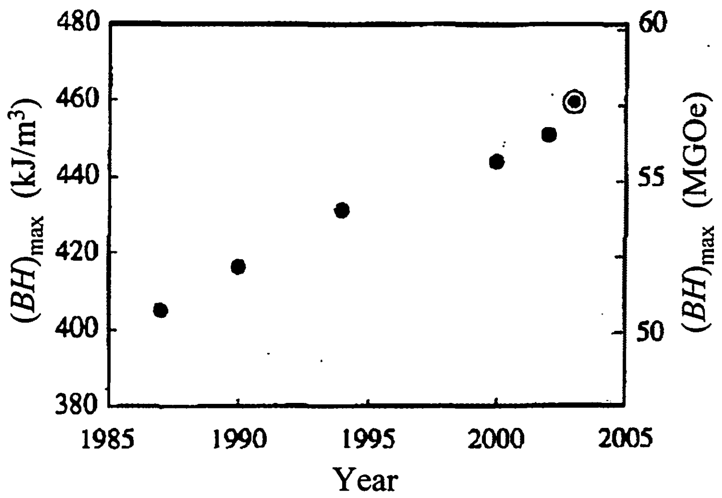

Fig. 1.2.1-2: Status of $(BH)_{max}$ of Nd-Fe-B sintered magnets [Kan04].

Enormous Nd-Fe-B permanent magnets are used in various types of motors and actuators in some industry applications, consumer electronics, and electronic devices, and absolutely contribute to the development of their miniaturization and high-power output. Permanent magnets are classified according to manufacturing process as major types [Edw01, Sag07, Taw05]: one is a sintered magnet, which has a high density of magnetic materials and high-performance magnetic characteristics; and the other is a bonded magnet, which has high mechanical strength and a great deal of flexibility in geometry. Recently, Nd-Fe-B sintered magnets are being increasingly used in motors as shown in Fig. 1.2.1-3, and are essential for the construction of electrical machines [Kan04]. In electronic devices such as computers, cameras, and cell-phones Nd-Fe-B bonded magnets, which have a great deal of flexibility are often applied [Joh97].

Figure 1.2.1-4 shows the production process of Nd-Fe-B sintered permanent magnets [Sag07]. The production process is classified as: powdering, forming, sintering, machining, surface treatment, and magnetization. In the sintering process, the formed powder is sintered at about 1100 °C, and contracts due to directional anisotropy, and therefore a machining process is required after the sintering process. Figure 1.2.1-5 shows the production process of Nd-Fe-B bonded permanent magnets, which does not include the machining process because there is no sintering process [Sag07].

In fact, permanent magnets should have a high heat resistance. The Curie temperature of Nd-Fe-B magnets is less than that of Sm-Co magnets. Furthermore, the coercive force of Nd-Fe-B magnets drastically decreases with an increase in temperature (–0.69 %/K in $Nd_{15}Fe_{77}B_8$ magnets). To compensate for heating resistance, Dy or Tb are substituted for part of the Nd, and Sm-Fe-N magnets, which have about the same saturation magnetic polarization M_s, a high Curie temperature T_c, and a high corrosion resistance are expected to be substituted for Nd-Fe-B magnets. The addition of Dy or Tb to Nd-Fe-B magnets, however, decreases the saturation magnetic polarization M_s, and it is difficult to manufacture Sm-Fe-N sintered magnets because the Sm-Fe-N materials dissolve into Sm-N and Fe at 600 °C [Oza08]. Hence, it is necessary to improve the magnetic characteristics of permanent magnets.

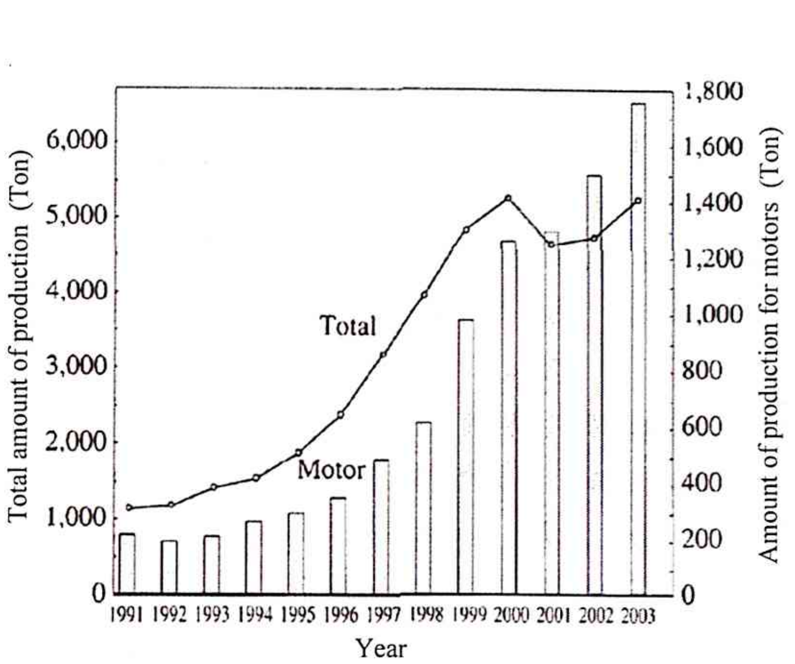

Fig. 1.2.1-3: Production of Nd-Fe-B sintered magnets for motors [Kan04].

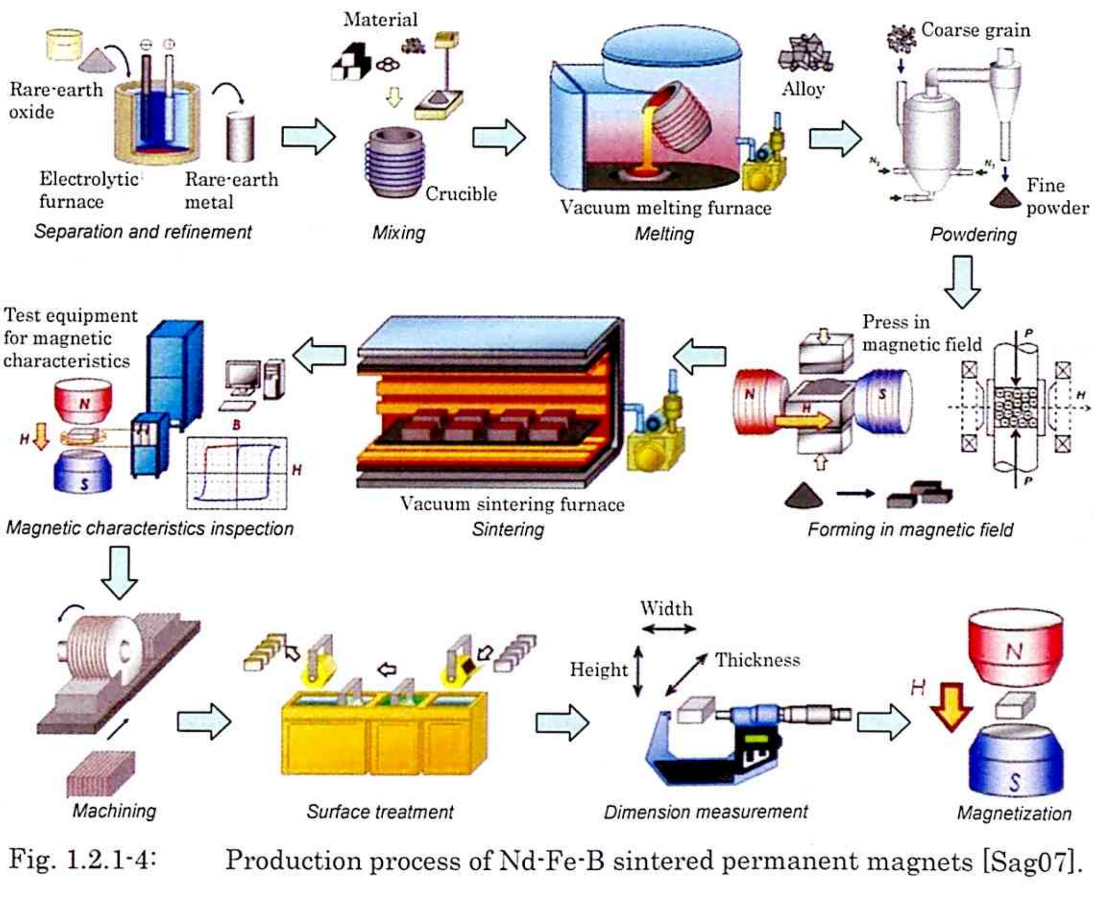

Fig. 1.2.1-4: Production process of Nd-Fe-B sintered permanent magnets [Sag07].

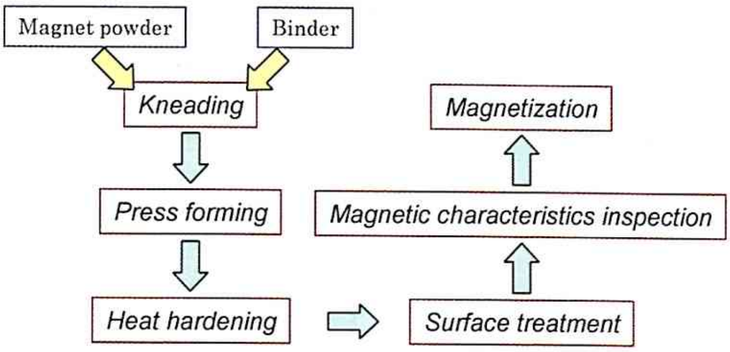

Fig. 1.2.1-5: Production process of Nd-Fe-B bonded permanent magnets [Sag07].

1.2.2. Magnetic Circuits

In MDOF actuators, the design of magnetic circuits, which involve magnetic materials, is absolutely essential in generating the MDOF driving forces. MDOF actuators have a magnetic circuit structure that basically extends the magnetic circuit of linear or rotary motors, and is based on drive principles such as stepping type, induction type, or synchronous type.

Stepping MDOF actuators can position a mover without position sensors, and were first put into practical use as drafting tools [MDD05]. Induction MDOF actuators have a simple, firm secondary conductor, and are being studied for application in transport switch systems in factories. Synchronous MDOF actuators offer good controllability of the driving forces, and therefore are being studied for use in the high-precision stages of semiconductor manufacturing, and in robot elements such as joints and eyes. Synchronous MDOF actuators often include permanent magnets to simplify and miniaturize their structure. Furthermore, to improve their drive performance in terms of such factors as speed and precision, synchronous MDOF actuators with a 2-D Halbach permanent-magnet array as shown in Fig. 1.2.2-1 have been studied. A Halbach permanent-magnet array generates a higher flux density and quasi-sinusoidal distribution with lower harmonic in the arranging direction than a NS permanent-magnet array does. Figure 1.2.2-2 shows the flux lines of NS and quasi-Halbach permanent-magnet arrays, and shows that the flux lines of the Halbach magnet array on one side are more densely and smoothly drawn than those of the NS magnet array [Jan07]. These Halbach magnetized actuators generate larger electromagnetic forces with less force ripples [How01].

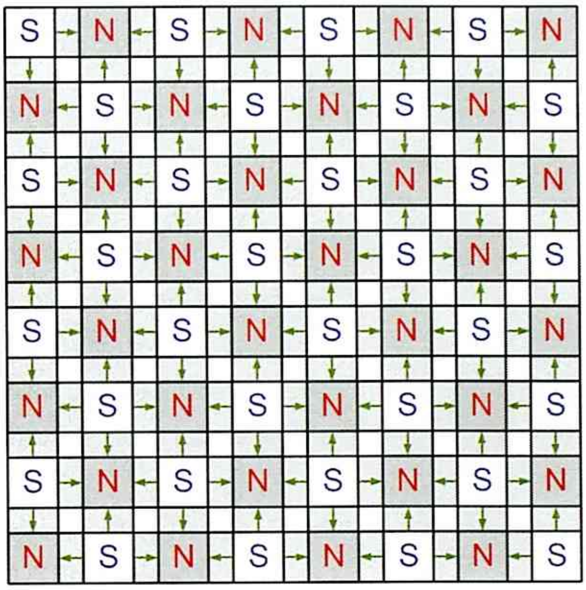

Fig. 1.2.2-1: 2-D Halbach permanent-magnet array.

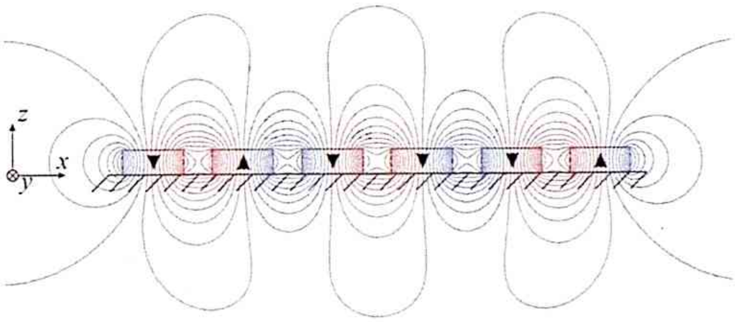

(a) Flux lines of a NS magnet array.

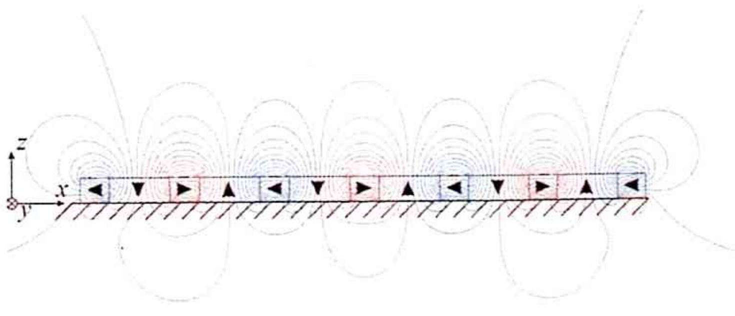

(b) Flux lines of a quasi-Halbach magnet array with two magnet segments per pole.

Fig. 1.2.2-2: Magnetic fields of Halbach and NS magnet arrays [Jan07].

1.2.3. Position-Sensing Systems

The MDOF position-sensing systems of a mover are of particular importance for high-performance motion control. To date, the following method of position sensing with MDOF have been used:

- Laser interferometer [Has01, HOh07, Kim97, Kim98, Tom94, Tom96].
- Combination of laser and photodetector [Ebi03, Ebi05, Ebi89, Ebi91, GKi01, GKi94, Ohi06].
- Magnetic sensor [Com03, Com04, Com07, Ish97, Hol98, Phi06].
- Inductive sensor or capacitance sensor [HOh07, Kim97, Kim98, Jan07, Van07a, Van07b].
- Optical encoder [Chi99, Don00, Don02, Kiy04, Kiy05a, Kiy05b, Nis07, Toy07, Toy95, Toy96, TSh06, Yan07].

In the high-precision stages of semiconductor manufacturing, for which planar actuators are mostly applied, position-sensing systems are required to measure the mover position with resolutions of several nanometers, and therefore often include multiple laser interferometers, as shown in Fig. 1.2.3-1 [Kim97]. In these applications, a position-sensing method with MDOF that utilizes a 2-D angle grid and a 2-D angle sensor, called a Surface Encoder, as shown in Fig. 1.2.3-2, is an emerging technology [Kiy04, Kiy05a, Kiy05b]. The surface of the 2-D angle grid installed on the mover is patterned three-dimensionally and cyclically. The five-degrees-of-freedom positions of the mover, which are the x–, y–, α–, β–, and γ–positions defined by Fig. 1.2.3-2, can be measured by detecting the diffraction pattern generated by irradiating the surface of the 2-D angle grid with multiple laser beams.

Some synchronous MDOF actuators with permanent magnets measure six-degree-of-freedom (6-DOF) mover positions by detecting the magnetic field using Hall elements, as shown in Fig. 1.2.3-3 [Com03, Com04, Com07]. Some variable reluctance-stepping-type planar actuators, often called Sawyer Motors, measure the x– and y–positions of the mover using multiple differential transformers, which are extremely easy to install in variable reluctance-stepping-type planar actuators, as shown in Fig. 1.2.3-4 [Hol98]. Most spherical actuators measure the mover position using optical encoders, as shown in Fig. 1.2.3-5 [Yan07].

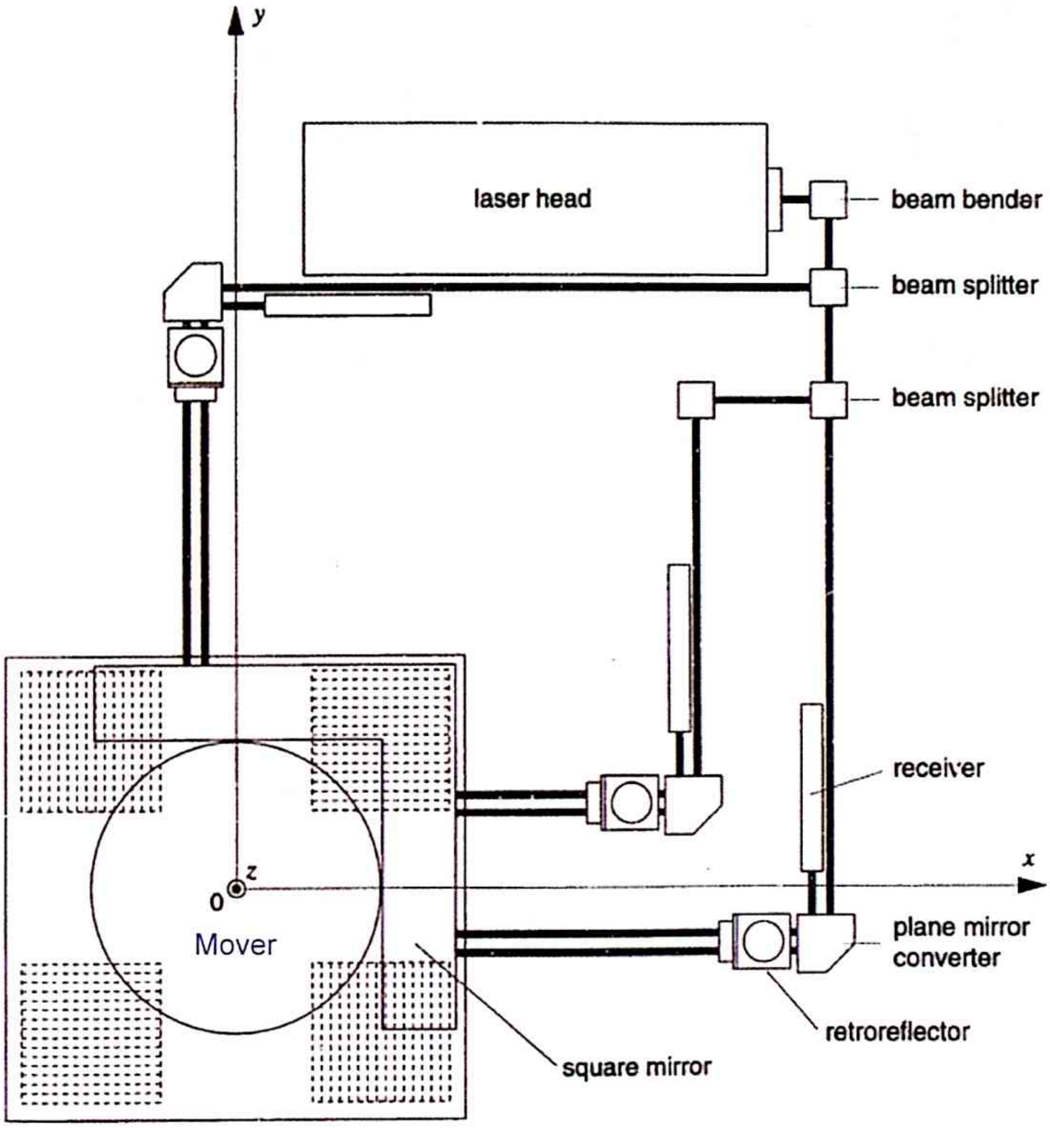

Fig. 1.2.3-1: Configuration of a position-sensing system using multiple laser interferometers [Kim97].

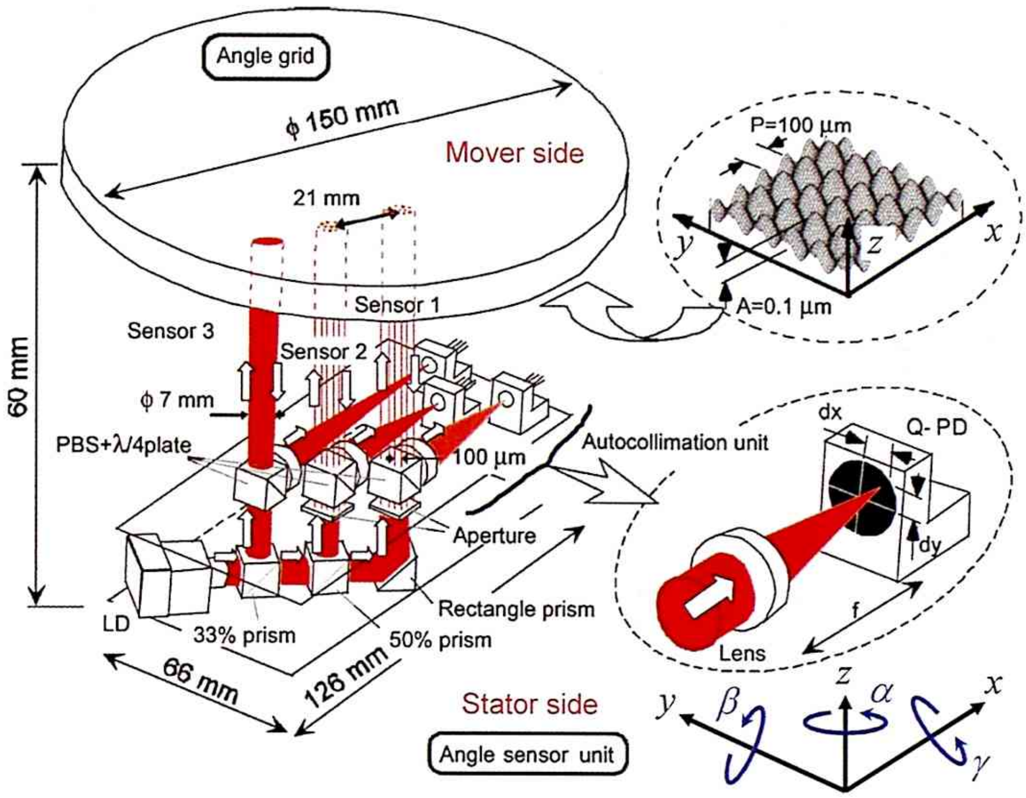

Fig. 1.2.3-2: Optical arrangement of a surface encoder [Kiy05].

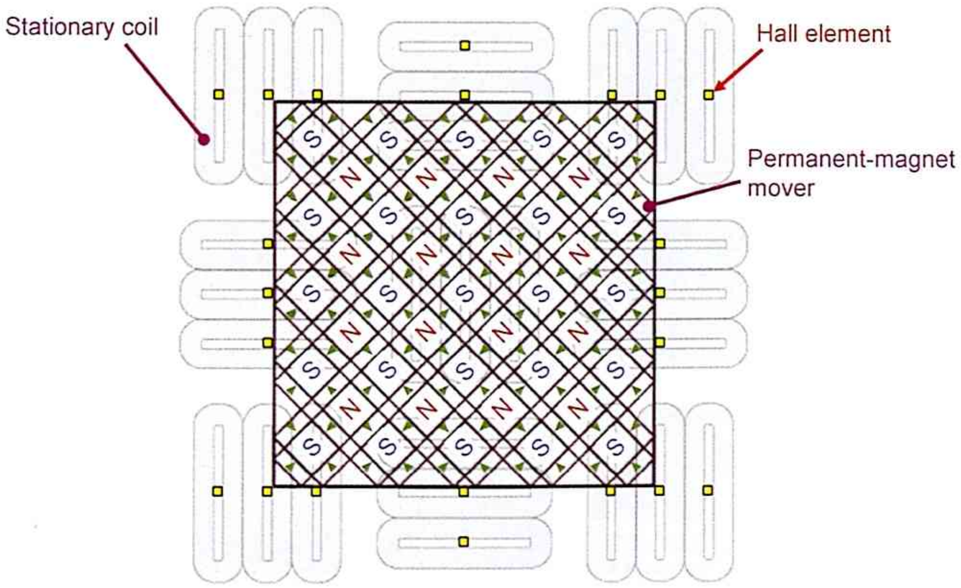

Fig. 1.2.3-3: Configuration of synchronous planar actuators with a position-sensing system that has multiple Hall elements [Com07, Jan07].

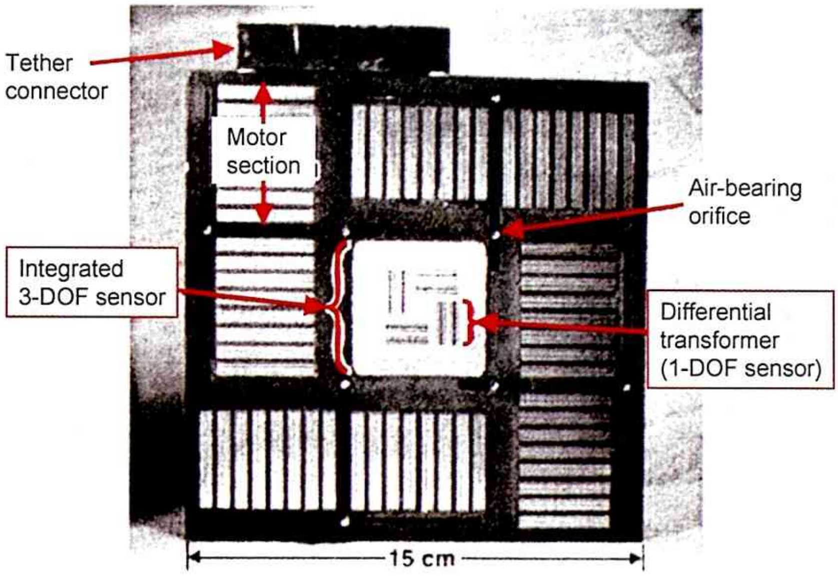

Fig. 1.2.3-4: Mover configuration of variable reluctance-stepping-type planar actuators with a position-sensing system that has multiple differential transformers [Hol98].

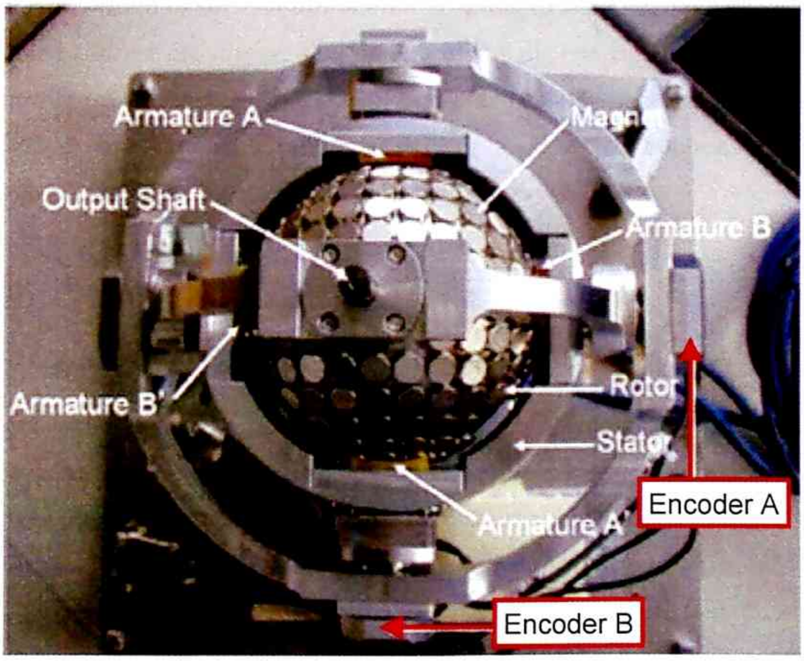

Fig. 1.2.3-5: Configuration of synchronous spherical actuators with a position-sensing system that has multiple optical encoders [Yan07].

1.2.4. Suspension and Guide Mechanisms

Suspension mechanisms, which guide a mover in the driving directions and suppress it in the other directions, are a particularly important part of MDOF actuators. So far, the following methods of suspension and guide for the mover have been used:

- Oil lubrication [Don00, Don02]
- Ball bearings [Chi99, Ebi89, Ebi91, GKi01, GKi94, Ohi98, Rau06, Yan07]
- Air bearings [Has01, Hol98, Kiy04, Kiy05a, Kiy05b, Ohi98, Saw68, Tsh06, Tom94, Tom96]
- Magnetic bearings [Com03, Com04, Com07, Hig90, HOh07, Kim05, Kim97, Kim98, Kor06, Kos04, Ohi06, Phi06, Tru06, Van06, Van07a, Van07b]

Oil lubrication on a contact surface between the stator and mover is extremely easy to realize, although it cannot be expected to smoothly drive the mover because of the viscosity resistance [MDD07]. Ball bearings are relatively easy to install in the stator or mover and they can suspend and guide the mover relatively smoothly [MDD07].

Contactless suspension of the mover by air bearings or magnetic bearings enables the mover to smoothly move because there is no friction between the mover and stator [MDD07]. Air suspension has a much higher stiffness at a shorter gap between the mover and stator, which is several μm/N on a 10-μm gap [Kiy04]. Therefore, air bearings are used in most planar actuators. The design of the air conduit and the compressor are extremely important parts of air bearings. Magnetic suspension requires not the design of an air conduit, but that of a magnetic circuit so that the suspension forces of the mover are generated without interfering with the driving forces.

1.3. Technical Issues with MDOF Actuators

MDOF actuators have three principally important element technologies: MDOF driving force generation, MDOF position sensing, and mover suspension and guides. Currently, the driving forces are generated multi-directionally, forming multiple magnetic circuits for unidirectional drive; mover positions are detected by a combination of position sensors for unidirectional displacement; and most movers are suspended and guided with ball bearings.

In most MDOF actuators that have been proposed, the magnetic circuits are all spatially separated from one another to make it easy to independently control the driving forces with each degree of freedom. The configuration of the magnetic circuits, however, often makes the movable area of the mover extremely narrow, unless numerous coils are used. If numerous coils were utilized to extend the movable area, then the power-supply system would become more complicated. In an MDOF position-sensing system that combines multiple-position sensors for unidirectional displacement, the measurable area, where all position sensors can measure each displacement, also is extremely narrow.

As stated above, the following improvements in MDOF actuators are required:

- Extension of the MDOF movable area without a complicated power-supply system.
- Extension of the measurable area with MDOF.

1.4. Contributions of this Thesis

This section presents the purpose of this study and the approach taken to this goal, and clarifies the assertions and contributions of this thesis.

1.4.1. Purpose of this Study

This study targets the design of driving force-generation mechanisms and motion-control systems of a planar actuator that has a mover capable of traveling over large displacements along a plane. In this study, to realize a high-performance drive for the mover, a planar actuator that has the following specifications is designed;

- decoupled control for 3-DOF motions on a plane.
- a wide movable area that can be extended regardless of the number of armature coils.
- ease of mover miniaturization.
- absence of problematic wiring that can hinder drive performance.
- a small number of armature currents to control.

First, to realize a planar actuator that can control the driving forces over a wide movable area, I have to design the planar actuator so that the movable area can be given, regardless of the number of the armature coils. For that purpose, I propose magnetic circuits that are not separated spatially due to overlapped armature conductors. The configuration of the magnetic circuits is the most novel feature in this study and enables the extension of the movable area by lengthening all the conductors, regardless of the number of conductors. However, the configuration of the magnetic circuits is not suitable for decoupled control of the MDOF driving forces because the magnetic fields, as a result of armature currents, are superimposed, and so a planar actuator with this type of magnetic circuit configuration has never been studied. This study asserts that it is possible to design a planar actuator so that the MDOF driving forces can be independently controlled using spatially superimposed magnetic circuits, and this assertion is the main contribution of this thesis.

Spatially superimposed magnetic circuits also allow the miniaturization of planar actuators, which was conventionally difficult. I see an application for this planar actuator for use as lens-driving-actuators in electronic devices, and this study involves the design of a planar actuator with a small mover—in the order of several tens of mm.

Finally, as a fundamental investigation of incremental improvements and to avoid deterioration of the drive characteristics caused by friction forces between the mover and stator, this study includes an investigation into the feasibility of magnetic suspension of the mover. This magnetically levitated planar actuator is defined as having six armature conductors, which is the minimum number of armature conductors needed to realize both magnetic suspension and planar motion control.

To perform an experimental verification of this planar actuator, I have to design the driving force-control system and position-sensing system with MDOF. In this study, the MDOF mover positions are detected using multiple laser-displacement sensors because of their fine precision. This sensing method gives a relatively wide measurable area, which is wide enough to investigate the drive characteristics of the proposed planar actuator.

1.4.2. Procedures used in Conducting this Study

This thesis presents an investigation into the feasibility of my targeted planar actuator by going through the following four, ordered stages;

(I) Conceptual Design of a Long-Stroke 3-DOF Planar Actuator:

In this stage, a planar actuator with spatially superimposed magnetic circuits for 3-DOF motion control is conceptually designed to drive the mover over a wide movable area on a plane by controlling only two pairs of three-phase currents. Then, the fundamental characteristics of the planar actuator are clarified and a 3-DOF decoupled motion-control system is designed.

(II) Design of an Experimental System for Verification of the Motion-Control Characteristics of the Planar Actuator:

In this stage, an experimental system for the verification of the motion-control characteristics of the planar actuator proposed in Stage (I) is designed, for example, the position-sensing system and the suspension and guide mechanisms. Specifications and characteristics of all the experimental apparatuses are described.

(III) Experimental Verification of the 3-DOF Motion-Control Characteristics of the Planar Actuator:

In this part, experiments on the motion-control characteristics of the planar actuator proposed in Stage (I) are conducted. There are two major experimental objectives: first, verification of decoupled control for the 3-DOF motion of the mover; and, second, investigation of the movable area of the mover in the yaw direction.

(IV) Feasibility Study on Planar Motion Control of the Planar Actuator with the Mover Magnetically Levitated:

In this stage, a planar actuator having the same configuration as the magnetic circuits for planar motion control is conceptually designed so that the mover can be magnetically suspended. The mover has 6-DOF motions (3-DOF translational and rotational motions), and so this stage introduces the 3-DOF translational and 1-DOF rotational motion-control system, which offers the other 2-DOF stable rotational motion, and an investigation of the motion-control characteristics by numerical analysis.

1.5. Thesis Overview

First of all, Chapter 1 comments upon the background and purpose of this study, and clarifies positions, assertions, and contributions of this thesis. Chapter 2 introduces previous techniques used in motion control with MODF, and comments upon their features and issues in detail. Chapter 3 presents fundamentally conceptual design of a long-stroke 3-DOF planar actuator. Chapter 4 presents the design of an experimental system for verification of the motion-control characteristics of the planar actuator. Chapter 5 describes experimental results of the motion-control characteristics of the planar actuator, and suggests incremental improvements to the planar actuator. Chapter 6 proposes conceptual design of the planar actuator with the same configuration of magnetic circuits for the planar motion control, so that the mover can be magnetically suspended, and presents a feasibility verification of the motion-control characteristics by numerical analysis. Finally, Chapter 7 concludes this thesis and suggests future work. Figure 1.5.0-1 shows the structure of this thesis.

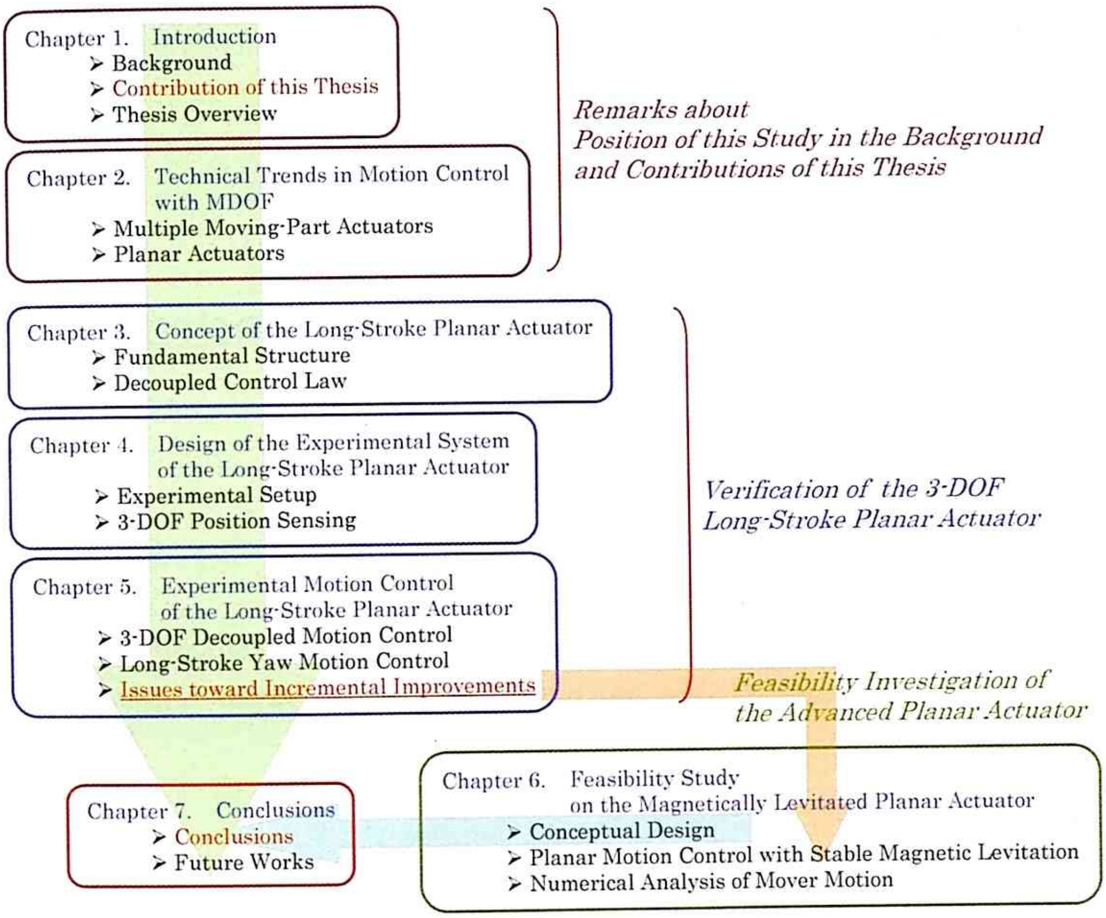

Fig. 1.5.0-1: Thesis structure.